

Comprehensive Analysis Reveals Biomarkers Related to Diabetic Peripheral Neuropathy and Its Molecular Mechanism

Qiujin Zhu^{1,2,*}, Shangheng Fan^{1,2,*}, Jingru Mou^{1,2}, Manlu Zhao^{1,2}, Changlu Li^{1,2}, Benben Yang^{1,2}, Yihan Shangguan^{1,2}, Xia Chen³, Yulan Cai¹⁻³

¹Department of Endocrinology, The Second Affiliated Hospital of Zunyi Medical University, Zunyi, 563006, People's Republic of China; ²Department of Endocrinology and Metabolism, The Affiliated Hospital of Zunyi Medical University, Zunyi, 563006, People's Republic of China; ³Department of Endocrinology, Kweichow Moutai Hospital, Renhuai, Guizhou, 564501, People's Republic of China

*These authors contributed equally to this work

Correspondence: Xia Chen; Yulan Cai, Email 736469203@qq.com; caiyulanuiui@163.com

Purpose: Diabetic peripheral neuropathy (DPN) is a common complication of both type 1 and 2 diabetes. DPN lacks accurate early diagnostic indicators, prompting united identification of biomarkers through transcriptomics and Mendelian randomization (MR) to inform DPN prevention and treatment strategies.

Patients and Methods: Differential expression analysis pinpointed DPN-related genes (DE-DPN-RGs) by screening differentially expressed genes (DEGs) across GSE95849 and GSE185011 datasets. MR approach validated DE-DPN-RGs causally linked to DPN as potential biomarkers, with sensitivity analysis and Steiger test reinforcing the findings. These biomarkers' expressions were verified via RT-qPCR, while their biological roles, pathways influencing DPN progression, and possible therapeutic targets were comprehensively investigated.

Results: 124 DE-DPN-RGs were identified from 5340 DEGs₁ and 896 DEGs₂, among them, *TNF*, *OSBPL8*, *IER3*, *SLC16A3*, *CREB5*, and *LRWD1*, showing significant causal relationships with DPN. Sensitivity analysis along with the Steiger test validated the reliability of the results, demonstrating their resilience against reverse causation. Furthermore, *OSBPL8*, *SLC16A3*, *CREB5*, and *LRWD1* demonstrated significant differential expression between DPN and control groups in both the GSE95849 and GSE185011 datasets, with consistent expression trends across both datasets, thereby warranting their designation as biomarkers. Biomarkers functioned in metabolic reactions of amino acids, rRNA processing, and translation, with potential therapeutic candidates including rosuvastatin, nitrofurfurylhydrazide, and neostigmine bromide. All four biomarkers exhibited significant upregulation in the DPN group as confirmed by RT-qPCR analysis, with the exception of *OSBPL8*, which displayed a non-significant difference between the groups.

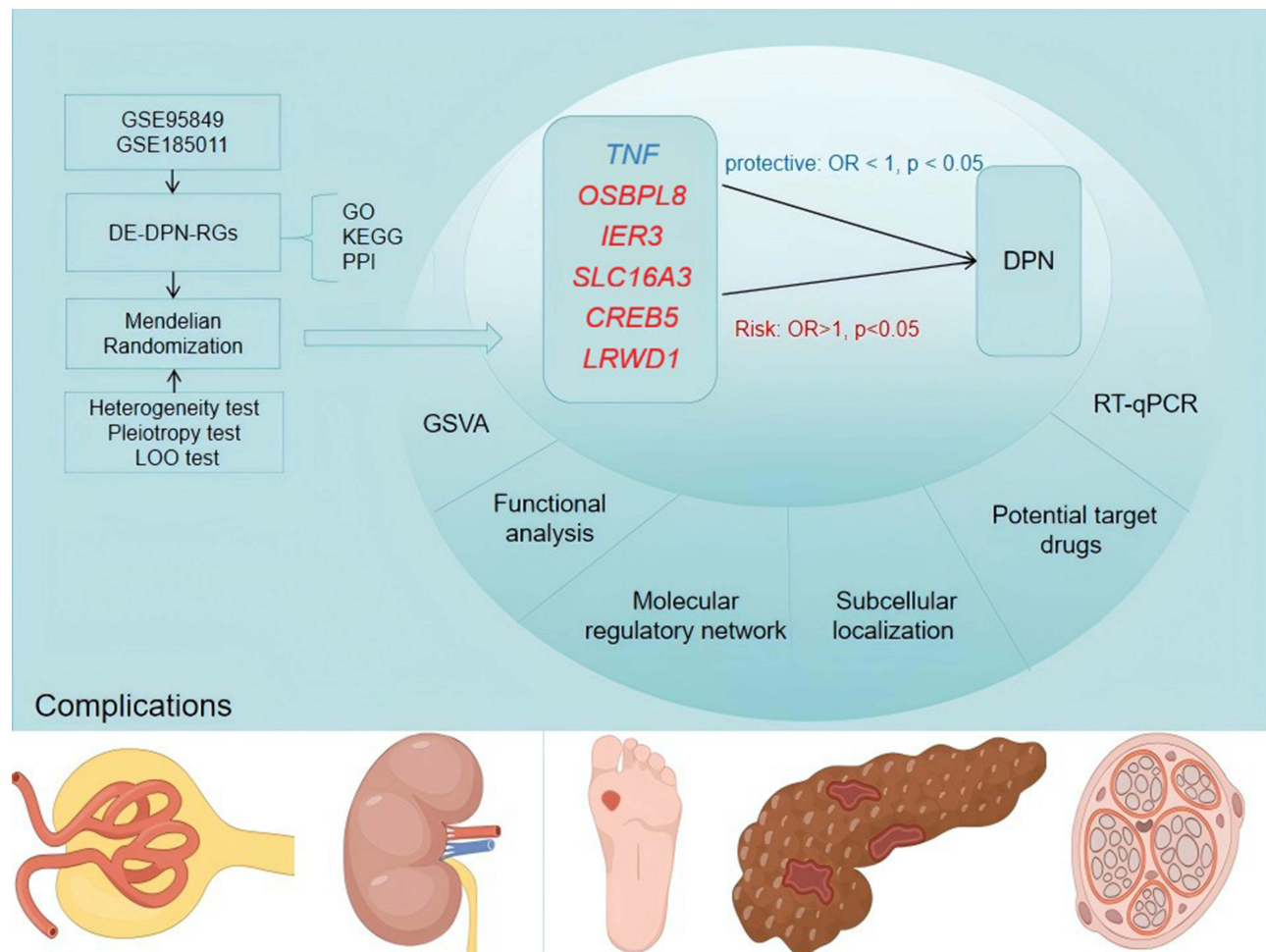
Conclusion: In conclusion, *SLC16A3*, *CREB5*, and *LRWD1* emerge as promising biomarkers, elucidating roles in DPN pathogenesis and offering potential therapeutic targets.

Keywords: diabetic peripheral neuropathy, mendelian randomization, biomarker, gene set enrichment analysis, drug prediction

Introduction

Globally, there is a concerning trend of the escalating prevalence rates and disease burden associated with diabetes, posing significant challenges to public health systems worldwide.¹ The International Diabetes Federation (IDF) diabetes map, published in 2021, reports that a staggering 536.6 million individuals worldwide afflicted with diabetes, constituting a prevalence of 10.5%.² Diabetic peripheral neuropathy (DPN) is one of the most common complications of diabetes, impacting approximately half of all individuals with diabetes.³ DPN manifests as a chronic, symmetrical, and progressive ailment typified by abnormal sensation or/and pain in its early stages. Patients frequently report lancinating, tingling, and burning sensations. These symptoms are often accompanied by depression, anxiety, and sleep disturbances.⁴ Due to the

Graphical Abstract



loss of peripheral nerve function, DPN initially affects the longest nerve fibers, with the condition subsequently progressing from distal to proximal regions.⁵ This progression can result in disability, severely diminishing the patient's quality of life and imposing substantial physical, emotional, and financial burdens on both the affected individuals and the healthcare system.⁶ Therefore, early and timely diagnosis and treatment of DPN are crucial in improving clinical outcomes and alleviating the economic and emotional burdens on patients. Currently, the diagnosis of DPN relies on nerve conduction studies (NCS), which is considered the gold standard.⁷ However, its time-consuming, labor-intensive, and notably expensive nature makes routine clinical application impractical.⁸ Considering the lack of precise early diagnostic markers for DPN, the existing ambiguity in our understanding of the underlying mechanisms of DPN and the scarcity of effective treatment strategies. There exists a compelling imperative to diligently pursue biomarkers for early detection and a comprehensive examination of the molecular mechanisms underlying these markers is imperative. It will further improve the diagnosis, treatment, and prognosis of this disease.

The Mendelian randomization (MR) methodology holds significant promise in evaluating causal relationships between exposures and outcomes in epidemiology.⁹ By utilizing genetic variants as instrumental variables (IVs) in non-experimental data, MR offers a robust approach to investigating such associations. Since genetic alleles are randomly arranged at conception and the germline genotype cannot be modified by disease, MR analyses are not biased by confounding between exposures and outcomes, reverse causality, or measurement error.¹⁰ Therefore, MR emerges as

a compelling approach for meticulously investigating the complex mechanisms involved in the pathogenesis of DPN. Most prior studies have employed MR to identify risk factors for DPN.^{11,12} However, fewer investigations focusing on the concurrent utilization of transcriptome analysis and MR in the study of DPN.

This study integrates transcriptome sequencing data of DPN in conjunction with MR analysis to scrutinize the correlation and causality between DEGs and the pathogenesis of DPN. This study will utilize enrichment analysis to investigate the relevant functional pathways and the pathogenesis of these genes. Furthermore, the validation of biomarker expression will be conducted using reverse transcription quantitative polymerase chain reaction (RT-qPCR). These comprehensive integrated methodologies, combining transcriptome sequencing data and MR analysis, are strategically crafted to unravel the intricate molecular mechanisms underlying the pathogenesis of DPN. By meticulously scrutinizing the correlation and causality between DEGs and DPN, these methodologies hold immense promise in unveiling novel therapeutic targets and paving the way for innovative interventions to ameliorate the burden of this debilitating condition.

Material and Methods

Statistical Collection of Data

The GSE95849 and GSE185011 datasets were obtained from the Gene Expression Ontology (GEO) database (<https://www.ncbi.nlm.nih.gov/geo/>).¹³ The GSE95849 dataset (GPL22448) was selected as the training set, wherein blood samples were obtained from six patients diagnosed with DPN and six control subjects.¹⁴ The GSE185011 dataset (GPL24676) served as the validation set, comprising blood samples obtained from five patients diagnosed with DPN and five normal control subjects.¹⁵ The integrative epidemiology unit open genome-wide association study database (IEU OpenGWAS, <https://gwas.mrcieu.ac.uk/>)¹⁶ was used to procure expression quantitative trait locus (eQTL) data for differentially expressed DPN-related genes (DE-DPN-RGs) which were employed as exposure factors in the MR analysis. The visit time was October 23, 2023. Simultaneously, a search was conducted by entering the keyword “diabetic neuropathy” in this database to obtain the “finn-b-DM_NEUROPATHY” dataset, utilized as the outcome. The dataset comprised 1,415 disease samples and 162,201 control samples, all sourced from European populations. The number of single nucleotide polymorphisms (SNPs) was 16,380,195.

Analysis of Differentially Expressed Genes (DEGs)

Gene expression data were extracted from DPN and normal control samples in the GSE95849 dataset. DEGs1 were then identified through screening using the “limma” (version 3.46.0)¹⁷ with $|\log_2\text{fold-change (FC)}| > 1$, *adj. p* < 0.05.¹⁸ Building upon this foundation, DEGs1 were visualized via the “ggplot2” (version 3.4.4)¹⁹ and the “pheatmap” (version 1.0.12) packages.²⁰ In addition, DEGs2 between DPNs and controls in the GSE185011 dataset were identified and visualized using the same methodology. Following this, the sets of DEGs identified in the GSE95849 and GSE185011 datasets were intersected to obtain the subset of differentially expressed DPN-related genes (DE-DPN-RGs).

Functional Enrichment Analysis of DE-DPN-RGs and Construction of a Protein-Protein Interaction (PPI) Network

The subset of differentially expressed DE-DPN-RGs underwent Gene Ontology (GO) and Kyoto Encyclopedia of Genes and Genomes (KEGG) enrichment analysis using the “clusterProfiler” package (version 4.4.4), with a significance threshold of *P* < 0.05.²¹ This analysis aimed to elucidate the biological functions and signaling pathways associated with the DE-DPN-RGs. Additionally, interactions among the DE-DPN-RGs at the protein level were investigated. The PPI network of the DE-DPN-RGs was constructed using the Search Tool for the Retrieval of Interacting Genes (STRING) database (<http://string-db.org>),²² with an interaction score threshold greater than 0.7, and visualized using “Cytoscape” software (version 3.8.2).²³

Selection of Instrumental Variables (IVs)

The following three assumptions were followed throughout the MR analysis: 1. The independence assumption (the causality between DE-DPN-RGs and DPN is independent of confounding factors); 2. The association assumption (there exists a robust correlation between IVs and DE-DPN-RGs); 3. The exclusivity assumption (DE-DPN-RGs represent the sole pathway through which genetic variation influences DPN).²⁴ Subsequently, IVs satisfying all three aforementioned assumptions were identified through screening. Initially, the `extract_instruments` function of the “TwoSampleMR” package (version 0.5.7).²⁵ It was employed to retrieve the differentially expressed DE-DPN-RGs and filter the IVs significantly correlated with the DE-DPN-RGs ($p < 5 \times 10^{-8}$). Subsequently, single nucleotide polymorphisms (SNPs) in linkage disequilibrium (LD) were excluded by the `Clump` function (`clump = TRUE`, $r^2 = 0.001$, $kb = 10,000$). After that, the number of SNPs was greater than 3 and the SNPs with F-values greater than 10 were reserved. The calculation formula for F values was as follows. In the formula, R^2 represents the cumulative explanatory variance of the selected SNPs, N represents the number of the samples.

$$F = \frac{R^2(n-2)}{1-R^2}$$

Following this, the `extract_outcome_data` function was utilized to retrieve the outcome data, and the IVs that were not relevant to the outcome was retained. SNPs meeting stringent screening criteria were then employed for subsequent MR analysis. Moreover, the `harmonise_data` function was applied to standardize effect alleles and effect sizes, ensuring consistency in allele representation between exposure factors and outcomes. Similarly, SNPs for multivariable Mendelian randomization (MVMR) analysis were selected using the aforementioned methodology.

Univariable MR (UVMR) Analysis

The univariable UVMR analysis of DE-DPN-RGs (exposure factors) and DPN (outcome) were performed to investigate the causal relationship between them. In UVMR analysis, inverse variance weighted (IVW) method²⁶ was employed as the primary approach, supplemented with the weighted median (WM),²⁷ MR Egger,²⁸ simple mode,²⁹ and weighted mode³⁰ methods. Notably, a p-value less than 0.05 from the IVW method indicated a significantly causal relationship between DE-DPN-RGs and DPN. Additionally, odds ratios (ORs) greater than 1 indicated that DE-DPN-RGs were risk factors for DPN, while ORs less than 1 indicated that DE-DPN-RGs were protective factors for DPN. Furthermore, the UVMR results were visualized using scatter plots, forest plots, and funnel plots.

Sensitivity Analysis

Subsequently, the reliability of the UVMR results was verified through sensitivity analyses. Firstly, a heterogeneity test was used to assess the presence of heterogeneity between the two datasets via the “TwoSampleMR”. If the p-value is greater than 0.05, there was no heterogeneity. If the results had heterogeneity ($P < 0.05$), random effects IVW was adopted in the MR, otherwise fixed effects IVW would be adopted. Secondly, the `mr_pleiotropy_test` function was utilized to assess whether there was horizontal pleiotropy between DE-DPN-RGs and the DPN dataset. In addition, the MR-PRESSO was used to correct for horizontal pleiotropy between them by removing outliers. If the p-value is greater than 0.05, it meant that there are no confounders and the results were trustworthy. The SNPs were then eliminated one by one using the leave-one-out (LOO) test to determine the effect of the remaining SNPs on the results.

MVMR Analysis

MVMR was further performed on the exposure factors screened by the UVMR analysis to determine if the exposure factors had a direct or indirect effect on DPN. Allelic effects and effect sizes were reconciled for DE-DPN-RGs and DPN data using the `mv_harmonise_data` function of “TwoSampleMR”. Unnecessary exposure factors were then removed using the `mv_lasso_feature_selection` function. Finally, the Steiger test was done to rule out the effect of reverse causation.

Identification of Biomarkers for DPN

Genes with a significantly causal relationship with DPN were screened as candidate biomarkers for DPN from DE-DPN-RGs based on UVMR analysis. In addition, the expression of candidate biomarkers in the GSE95849 and GSE185011 datasets was examined and validated. Ultimately, candidate biomarkers with significant expression differences between DPN and controls and consistent expression trends in both datasets could be used as biomarkers for DPN.

Functional Analysis of Biomarkers

In the GSE95849 dataset, the samples were divided into high and low expression groups based on the expression of biomarkers, and the genes between them were analyzed for differences, and $|\log_2FC|$ of each gene was calculated and ranked from largest to smallest. The biomarkers were then subjected to gene set enrichment analysis (GSEA)³¹ using the “clusterProfiler” (version 4.7.1.003).³² The reference gene set was the background gene set “c2.all.v7.2.symbols.gmt” from the Molecular Signatures Database (MSigDB)³³ ($P < 0.05$). To explore differential biological pathways between high and low expression groups of biomarkers, gene set variation analysis (GSVA) was performed on different expression groups based on the “c2.all.v7.2.symbols.gmt” ($P < 0.05$). In addition, the co-expression network of biomarkers and other functionally similar genes was explored using GeneMANIA (<http://genemania.org/>). In addition, functional similarities between biomarkers were analyzed with the help of the “GOSemSim” (version 2.24.0)³⁴ (functional similarity score > 0.5).

Subcellular Localization and N⁶-Methyladenosine Binding Site Prediction

The localization of the biomarkers in subcells was predicted with the help of the mRNALocator online website (<http://bio-bigdata.cn/mRNALocator>).³⁵ The localization scores of the biomarkers in different subcells were calculated. Next, the occupancy of the biomarkers in different subcells was plotted based on this score. To explore whether N⁶-methyladenosine (m⁶A) affected the translational stability of biomarkers, the biomarker m⁶A binding sites were predicted. First, genome sequence for the biomarkers were obtained at National Center for Biotechnology Information (NCBI, <https://www.ncbi.nlm.nih.gov/>).³⁶ Then the m⁶A binding sites of the biomarkers were predicted from the sequence-based RNA adenosine methylation site predictor database (SRAMP, <http://www.cuilab.cn/sramp>).³⁷

Construction of Biomarker Regulatory Networks

In order to investigate the regulatory mechanisms of biomarkers at the molecular level, the miRDB database (<http://mirdb.org>)³⁸ and TargetScan database (<http://www.targetscan.org>)³⁹ were used to predict the upstream miRNAs corresponding to biomarkers. And miRNAs were then obtained by taking the intersection of the predictions from the two databases. After that, the upstream lncRNAs of the miRNAs were predicted using the Starbase database (<https://starbase.sysu.edu.cn/>).⁴⁰ In addition, a competing endogenous RNA (ceRNA) regulatory network was constructed using the “Cytoscape”. Potential transcription factors (TFs) for biomarkers were predicted in the Human Transcription Factor Targets database (hTFtarget, <http://bioinfo.life.hust.edu.cn/hTFtarget/>).⁴¹ Next, the TF-mRNA-miRNA network was mapped using the “Cytoscape”.

Prediction of Drugs for DPN-Targeted Therapies

The Drug Signatures Database (DsigDB, <http://tanlab.ucdenver.edu/>),⁴² an online database, was used to predict the targeted drugs associated with the biomarkers, and the targeting relationships between the biomarkers and drugs were demonstrated using “Cytoscape”.

Expression Analysis of Biomarkers

For validating the expression of biomarkers, reverse transcription quantitative polymerase chain reaction (RT-qPCR) was performed on 5 DPN and 5 control samples from peripheral blood mononuclear cell (PBMC). The blood samples used in this study were obtained from the Second Affiliated Hospital of Zunyi Medical University, with sample collection

occurring between December 2023 and April 2024. All subjects provided informed consent prior to participation. The collection process adhered to the ethical standards set by the Medical Ethics Committee of Zunyi Medical University. The amplification conditions for RT-qPCR were 40 cycles with 1 minute at 95°C, 20 seconds at 95°C, 20 seconds at 55°C, and 30 seconds at 72°C. The qPCR primers were listed in [Table S1](#) with GAPDH as reference gene. The relative expression levels of biomarkers were calculated using the $2^{-\Delta\Delta CT}$ method.

Statistical Analysis

The R programming language (version 4.2.1) was engaged in statistical analysis. Wilcoxon test was utilized to examine the discrepancies between 2 groups. $P < 0.05$ was considered notably significant. If not specified, *adj. P* < 0.05 or $P < 0.05$ indicates significant differences.

Results

The Biological Functions of 124 DE-DPN-RGs

Among 5,340 DEGs identified between DPN and controls in the GSE95849 dataset, 3,746 DEGs exhibited upregulation, while 1,594 DEGs demonstrated downregulation. The distribution of these DEGs¹ was visualised using a volcano and a heatmap ([Figure 1A](#) and [B](#)). A total of 896 DEGs² were identified between DPN and controls in the GSE185011 dataset, with 823 DEGs² were up-regulated and 73 DEGs² were down-regulated ([Figure 1C](#) and [D](#)). The intersection of the 3,746 DEGs from the GSE95849 dataset with the 896 DEGs from the GSE185011 dataset yielded a total of 124 DE-DPN-RGs ([Figure 1E](#)). Additionally, DE-DPN-RGs were significantly enriched in several biological functions, including the “intrinsic apoptotic signaling pathway”, “cell chemotaxis”, “regulation of neuron death”, “positive regulation of cytokine production”, “positive regulation of interleukin-6 production”, and “Toll-like receptor binding” ($P < 0.05$) ([Figure 1F](#)). In the KEGG analysis, DE-DPN-RGs were significantly enriched in the “TNF signaling pathway”, “Toll-like receptor signaling pathway”, “Antifolate resistance”, and “African trypanosomiasis” ($P < 0.005$) ([Figure 1G](#)). Furthermore, a robust linkage among these 124 DE-DPN-RGs was demonstrated in the PPI network, with prominent interactions observed among genes *TNF*, *HIF1A*, *NOD2*, and *SAMD9L* ([Figure 1H](#)).

TNF, *OSBPL8*, *IER3*, *SLC16A3*, *CREB5*, and *LRWD1* Were Significantly and Causally Associated with DPN

A total of six DE-DPN-RGs causally associated with DPN were screened as candidate biomarkers for DPN. Among them, *TNF* was a protective factor for DPN ($OR < 1$, $P < 0.05$). *OSBPL8*, *IER3*, *SLC16A3*, *CREB5*, and *LRWD1* were risk factors for DPN ($OR > 1$, $P < 0.05$) ([Figure 2A](#)). The scatter plot further demonstrated this result. *TNF* had a negative slope and was a protective factor for DPN, whereas *OSBPL8*, *IER3*, *SLC16A3*, *CREB5*, and *LRWD1* had positive slopes and were risk factors for DPN ([Figure S1](#)). The results based on the IVW algorithm showed that the distribution of SNP loci for the diagnostic efficacy of DPN in the data of *TNF* was all less than zero in the forest plot, which further suggested that *TNF* was protective factor for DPN. In contrast, the distribution of SNP loci diagnostic of DPN efficacy in the *OSBPL8*, *IER3*, *SLC16A3*, *CREB5*, and *LRWD1* data were all greater than zero, which further suggested that all of these genes were risk factors for DPN ([Figure S2](#)). SNPs were uniformly and randomly distributed on both sides of the IVW line, suggesting that the analyses followed Mendel’s second law ([Figure S3](#)).

The results of the heterogeneity test indicated that there was no heterogeneity between the DE-DPN-RGs (*OSBPL8*, *SLC16A3*, *CREB5*, *LRWD1*, and *TNF*) dataset and the DPN dataset ($p > 0.05$). Although the p-value of *IER3* was less than zero, the heterogeneity did not affect the results too much due to the IVW algorithm used ([Table 1](#)). Moreover, the results of the horizontal polytropy test proved that there was no influence of confounding factors in the analysis of this study ($p > 0.05$) ([Table 2](#)). Also, MR-PRESSO results confirmed the absence of horizontal pleiotropy between them ([Table 3](#)). Then, in the causal relationship between these six candidate biomarkers and DPN did not change significantly by excluding a SNP, which confirmed the stability of the result ([Figure S4](#)). Additionally, the six candidate biomarkers passed the Steiger test ($p < 0.0001$), confirming the reliability of the forward analysis of causality ([Table 4](#)). Finally, the

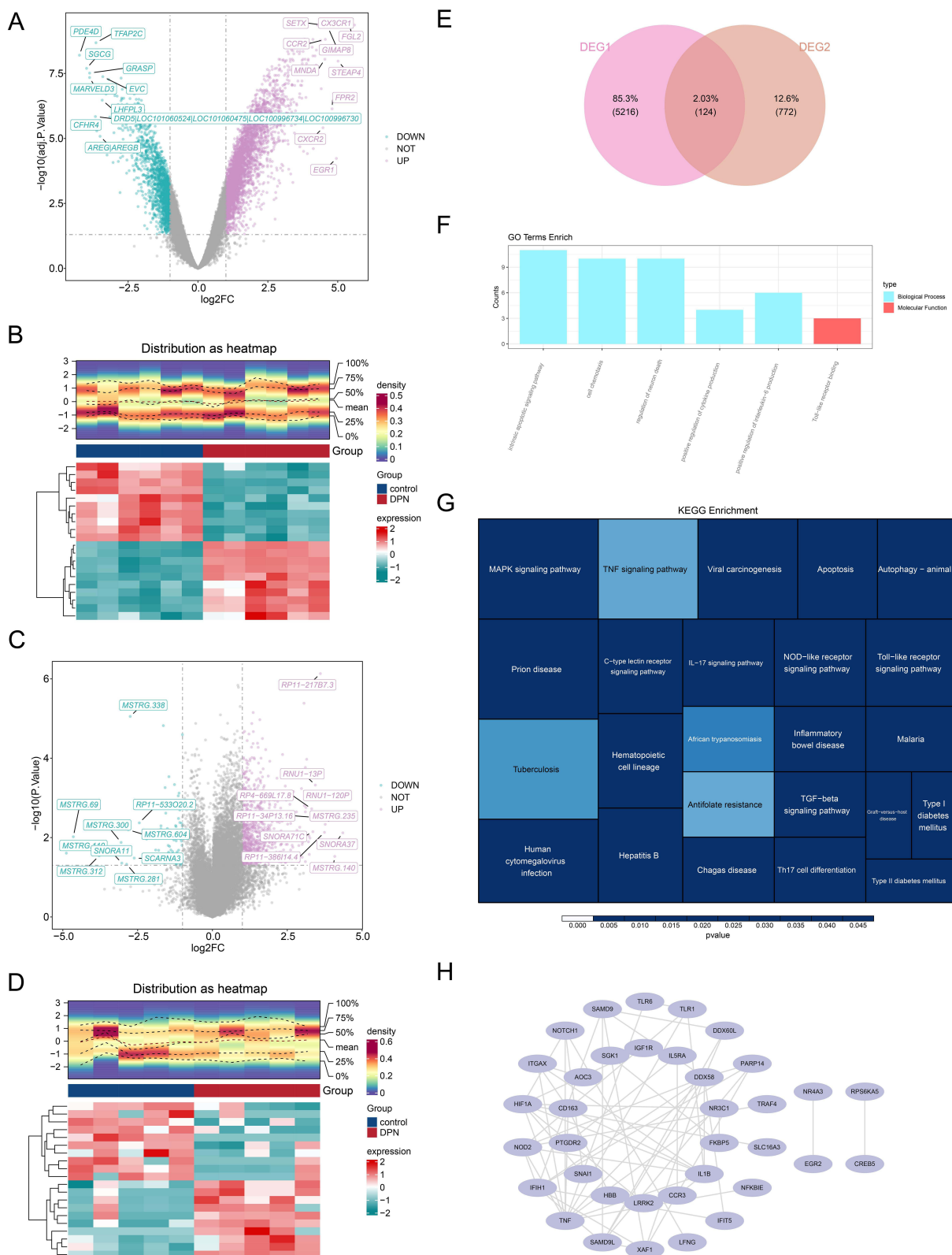


Figure 1 Results of differential expression analysis. **(A)** The volcano plot of differential genes in the GSE95849 dataset, with blue representing down-regulated genes and purple representing up-regulated genes; **(B)** The heatmap plot of differential genes in the GSE95849 dataset; **(C)** The volcano plot of differential gene expression in the GSE185011 dataset; **(D)** The heatmap plot of differential genes in the GSE185011 dataset; **(E)** The Venn diagrams for DEG1 and DEG2; **(F)** Results of GO enrichment analysis ($P < 0.05$); **(G)** Results of KEGG enrichment analysis ($P < 0.005$); **(H)** Results of PPI network.

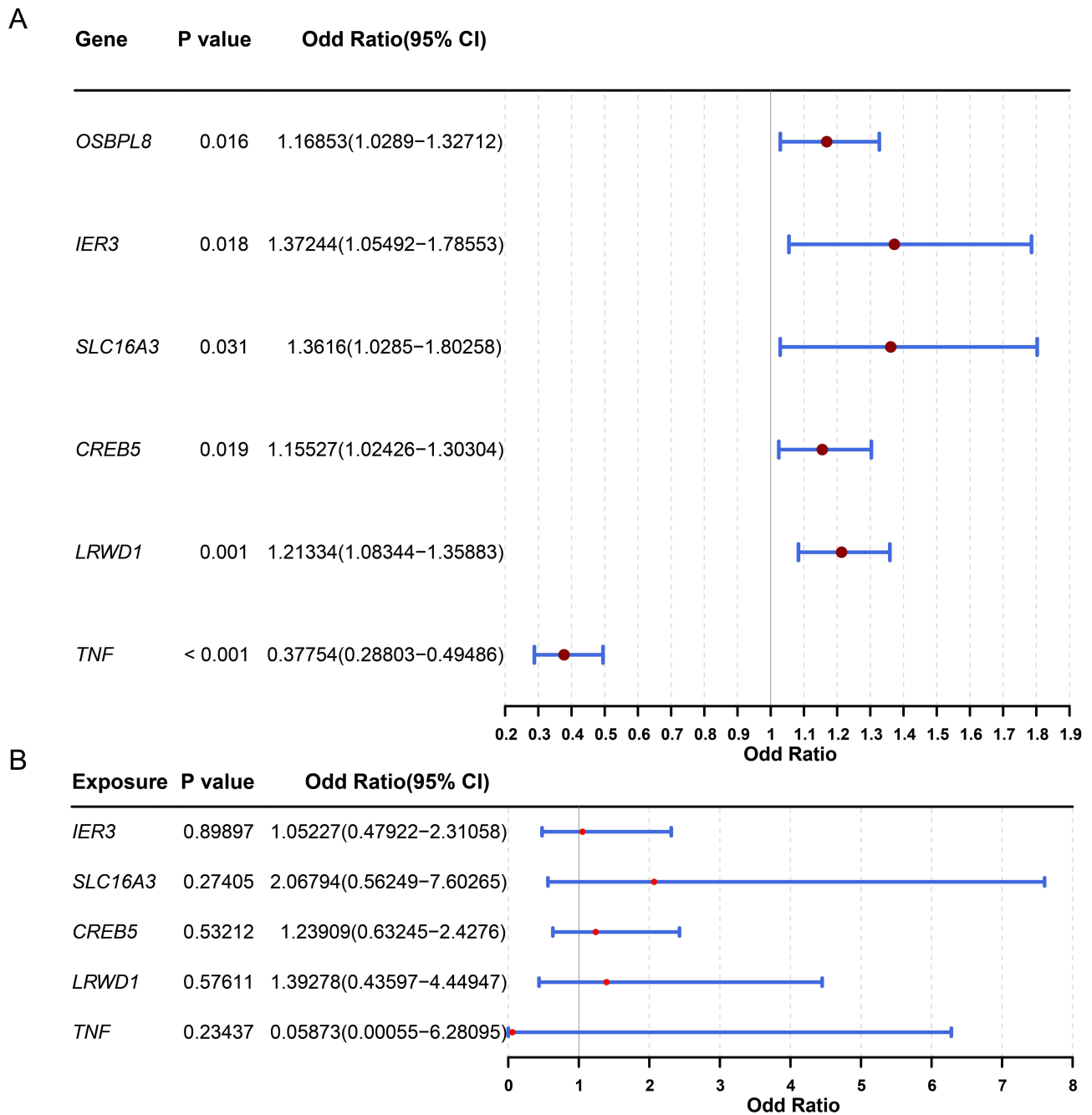


Figure 2 The forest map of candidate biomarkers. (A) Six DE-DPN-RGs exhibit causal associations with DPN; (B) Results of multifactorial Mendelian randomisation analysis.

results of the MVMR analysis showed that *TNF* remained a protective factor for DPN, and *OSBPL8*, *IER3*, *SLC16A3*, *CREB5*, and *LRWD1* remained risk factors for DPN (Figure 2B).

CREB5, *LRWD1*, *OSBPL8*, and *SLC16A3* Were Biomarkers of DPN

Validation in the GSE185011 dataset showed that the expression levels of *CREB5*, *LRWD1*, *OSBPL8*, and *SLC16A3* were significantly different between DPN and controls, with consistent trends in the GSE95849 dataset, and that they were upregulated in DPN (Figure 3A and B). Therefore, these four genes were credited as biomarkers of DPN. Subsequently, the GSEA results demonstrated the signaling pathways in which the biomarkers were involved. GSEA results showed

Table 1 Results of MR Heterogeneity Test Analysis

Symbol	Method	Q	Q_df	Q_pval
<i>OSBPL8</i>	Inverse variance weighted	1.051983269	2	0.591
<i>IER3</i>	Inverse variance weighted	23.22206565	8	0.003
<i>SLC16A3</i>	Inverse variance weighted	5.526523367	2	0.063
<i>CREB5</i>	Inverse variance weighted	3.654223572	6	0.723
<i>LRWD1</i>	Inverse variance weighted	7.836448415	8	0.45
<i>TNF</i>	Inverse variance weighted	0.286888865	2	0.866

Abbreviation: Q, Q statistic.

Table 2 Results of MR Level Multiple Validity Test Analysis

Symbol	Egger_Intercept	se	pval
<i>OSBPL8</i>	-0.013181013	0.036788631	0.780976512
<i>IER3</i>	0.060695183	0.051177691	0.274324646
<i>SLC16A3</i>	0.061311135	0.086950095	0.609013129
<i>CREB5</i>	0.033441884	0.032124339	0.34556537
<i>LRWD1</i>	-0.045083011	0.035990422	0.250561618
<i>TNF</i>	0.044648237	0.0985912	0.729289119

Abbreviations: Se, Standard errors of beta; pval, P-value.

Table 3 Results of the Analysis of the MR-PRESSO Horizontal Multiple Validity Test

Id. Exposure	Symbol	MR.Analysis	RSSobs	Pvalue
eqtl-a-ENSG00000146592	<i>CREB5</i>	Raw	5.890557345	0.5
eqtl-a-ENSG00000146592	<i>CREB5</i>	Outlier-corrected	5.890557345	0.5
eqtl-a-ENSG00000161036	<i>LRWD1</i>	Raw	8.103840776	0.5
eqtl-a-ENSG00000161036	<i>LRWD1</i>	Outlier-corrected	8.103840776	0.5

Table 4 Reverse Causality Analysis

ENSEMBL	Symbol	Correct_Causal_Direction	Steiger_pval
eqtl-a-ENSG00000091039	<i>OSBPL8</i>	TRUE	1.44E-229
eqtl-a-ENSG00000137331	<i>IER3</i>	TRUE	0
eqtl-a-ENSG00000141526	<i>SLC16A3</i>	TRUE	2.66E-196
eqtl-a-ENSG00000146592	<i>CREB5</i>	TRUE	0
eqtl-a-ENSG00000161036	<i>LRWD1</i>	TRUE	0
eqtl-a-ENSG00000232810	<i>TNF</i>	TRUE	4.89E-95

that the signaling pathways co-enriched by these four biomarkers were “metabolic reaction groups of amino acids and derivatives”, “rRNA processing”, and “translation” (Figure 3C–F).

Functions and Functional Associations of Biomarkers

GSVA results showed significantly different biological pathways. Among them, “reactive protein NF-kb activation through fadd rip 1 pathway bmediated by caspase 8 and 10”, “biocarta spps pathway” and “reactome clec7a dectin 1 induces nfat activation” were significantly highly expressed in the high expression group. For example, signaling pathways such as “reactome phospholipase c mediated cascade FGFR4”, and “NF-kb is activated and signals survival”, “PI3K cascade FGFR3”, were significantly highly expressed in the low expression group (Figure 4A–D). The GeneMANIA results showed

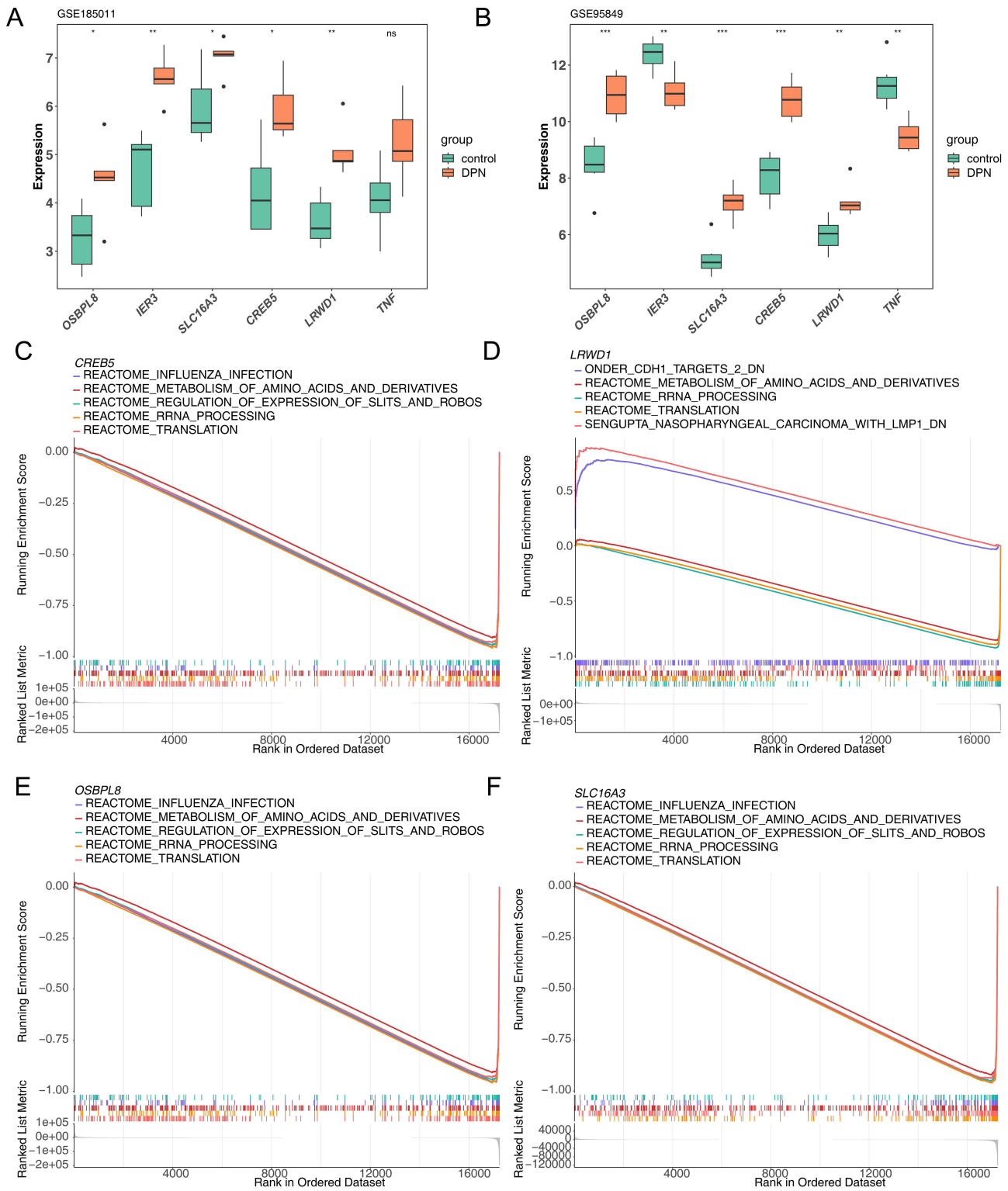


Figure 3 The results of expression validation analyses and GSEA enrichment analyses. The expression results of biomarkers in GSE185011 dataset (**A**) and GSE95849 (**B**); *: $P < 0.05$, **: $P < 0.01$, ***: $P < 0.001$, ns, no significance. The results of GSEA analysis of four biomarkers (**C–F**).

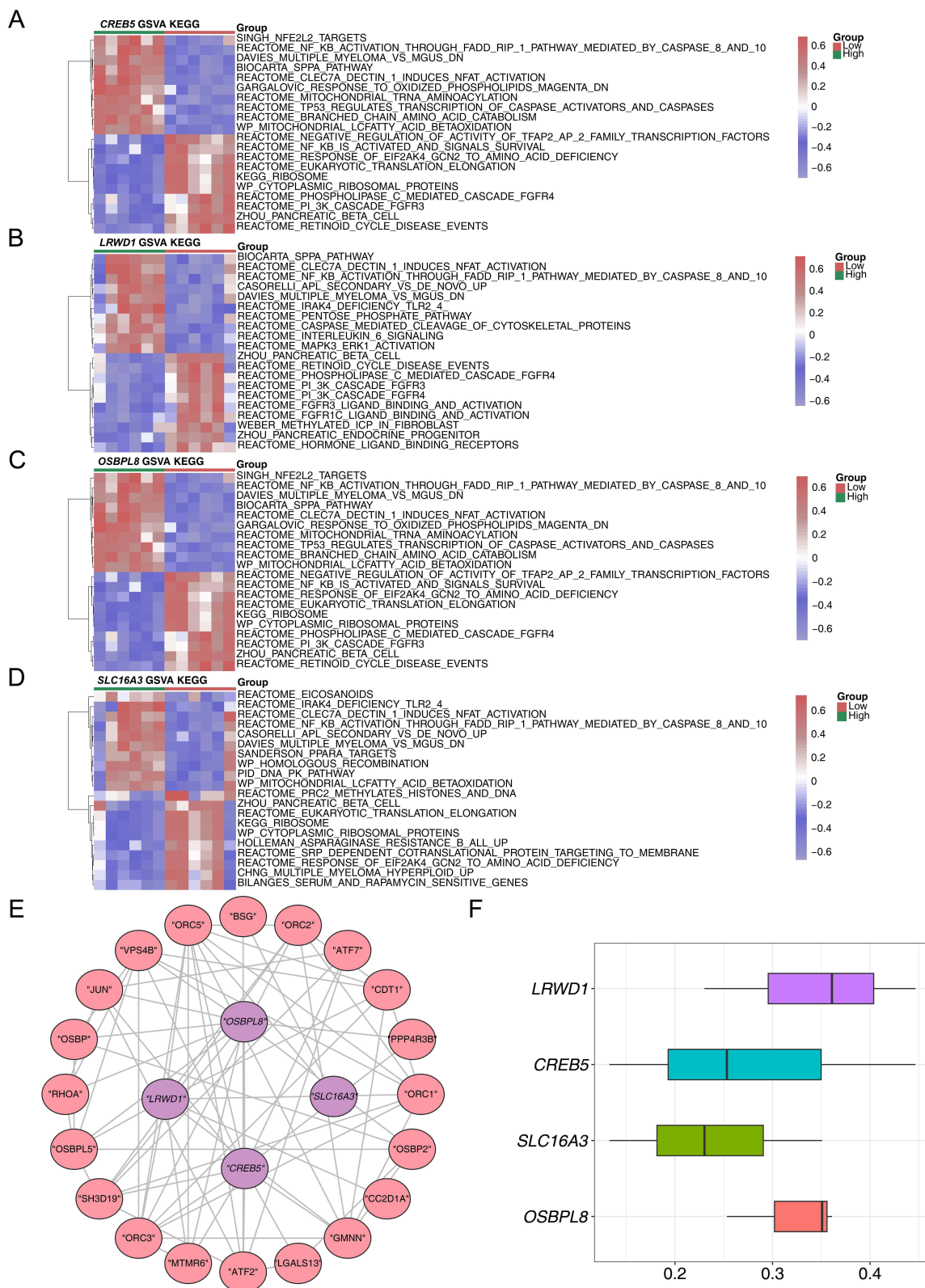


Figure 4 The GWSA enrichment analysis and GeneMANIA database analysis. **(A–D)** The Heatmap of GWSA analysis of four biomarkers; **(E)** The GeneMANIA analysis results; **(F)** The Results of Florends analysis.

that there were various relationships between biomarkers and other genes such as co-expression, the same location, physical interactions, genetic interactions, sharing protein structural domains, or participating in the same pathway. Among them, *LRWD1* interacted most closely with *ORC5* and *ORC2* (Figure 4E). Furthermore, the results of the Friends analysis demonstrated a low functional similarity between the four biomarkers (functional similarity score < 0.5) (Figure 4F).

Subcellular Localization of Biomarkers and Where Biomarkers Undergo m⁶A Methylation

SLC16A3, *CREB5* and *LRWD1* were detected in the cytoplasmic region, whereas *OSBPL8* was detected as up-regulated in the extracellular region. *SLC16A3* was also detected in the endoplasmic reticulum (Figure 5A). Meanwhile, the predicted locations of biomarkers susceptible to m⁶A methylation showed that *CREB5* was more susceptible to m⁶A methylation at positions 0 to 1000 of the base (Figure 5B). *LRWD1* was prone to m⁶A methylation at about 1000, 1500, and 2000 base positions (Figure 5C). *SLC16A3* was found to be susceptible to m⁶A methylation at around 1500 to 2000 base positions (Figure 5D). *OSBPL8* was susceptible to m⁶A methylation at around 60 base positions (Figure 5E).

Molecular Regulatory Network of DPN and Its Potential Target Drugs

A total of 54 miRNAs were obtained by taking the intersection of the two database predictions. A total of 759 lncRNAs were predicted based on 54 miRNAs. Based on this, a ceRNA network was constructed with *OSBPL8* and *CREB5* (Figure 6A). Meanwhile, *CREB5* and *OSBPL8* predicted 28 TFs and 20 TFs, respectively, and a TF-mRNA-miRNA regulatory network was constructed by combining the predicted miRNAs (Figure 6B). Where *PBX3*, *ETS1*, *EP300*, *CREBBP*, and *BRD4* were TFs predicted by *CREB5* and *OSBPL8*. In addition, there are 43 targeted drugs available for DPN treatment (Figure 6C). Examples included rosuvastatin, nitrofurfurylhydrazine, and neostigmine bromide.

All Four Biomarkers Were Highly Expressed in the DPN Group by RT-qPCR

As verified by RT-qPCR, the expression levels of *CREB5*, *LRWD1*, *OSBPL8*, and *SLC16A3* were higher in the DPN group, which was consistent with the trend in the GSE185011 and GSE95849 datasets, with only *OSBPL8* showing a non-significant difference between groups (Figure 7).

Discussion

As one of the most prevalent complications of diabetes, DPN significantly impairs patients' quality of life.⁴³ The therapeutic efficacy of DPN is often suboptimal, and the treatment duration is typically prolonged. Therefore, early diagnosis plays a pivotal role in facilitating timely treatment initiation, which in turn contributes to achieving favorable treatment outcomes, and alleviating the associated economic burden. However, the absence of precise indicators for early DPN detection has hindered the development of accurate diagnostic modalities.⁸ In this study, we identified six candidate biomarkers, *TNF*, *OSBPL8*, *IER3*, *SLC16A3*, *CREB5*, *LRWD1* through transcriptomics and MR techniques. We found that *TNF* is a protective factor for DPN. Conversely, the remaining five genes were identified as risk factors for the development of DPN. To enhance the stability and reliability of our findings, we conducted expression validation analyses for these six candidate biomarkers. Among them, the four candidate biomarkers with significant expression and the same trend between the training and validation sets were recorded as the biomarkers: *OSBPL8*, *SLC16A3*, *CREB5*, and *LRWD1*. Additionally, elucidating the molecular mechanisms holds paramount importance for advancing clinical research on DPN and enhancing our understanding of its pathogenesis.

OSBPL8, belonging to the oxysterol-binding protein-like (OSBPL) family, serves as a crucial intracellular lipid binding and transport protein involved in lipid transportation and cholesterol level regulation.⁴⁴ OSBP-related protein 8 (ORP8), encoded by *OSBPL8*, is targeted for silencing by miR-143, a micro-RNA associated with obesity, diabetes and cancer.⁴⁵ Decreased expression of ORP8 in cultured hepatocytes has been shown to impair insulin-induced AKT activation. Furthermore, induced transgenic overexpression of miR-143 impairs insulin-stimulated AKT activation and glucose homeostasis, suggesting that the miR-143-ORP8 pathway may represent a potential target for obesity-associated

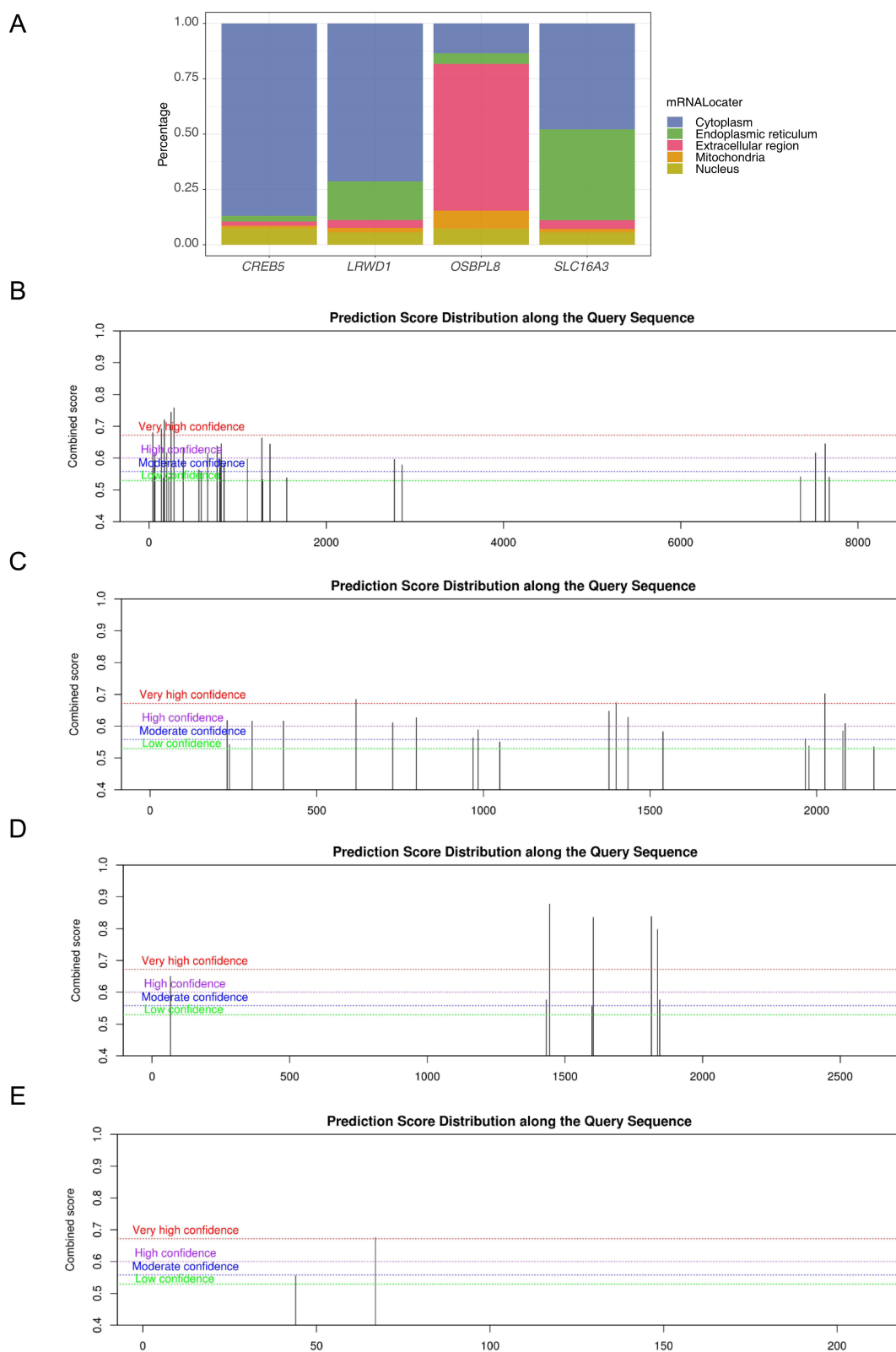


Figure 5 The results of subcellular localisation and m6A binding site prediction of key genes. **(A)** Subcellular localisation results for biomarkers; The results of methylation analysis of four biomarkers, **(B)** *CREB5* **(C)** *LRWD1* **(D)** *SLC16A3* **(E)** *OSBPL8*.

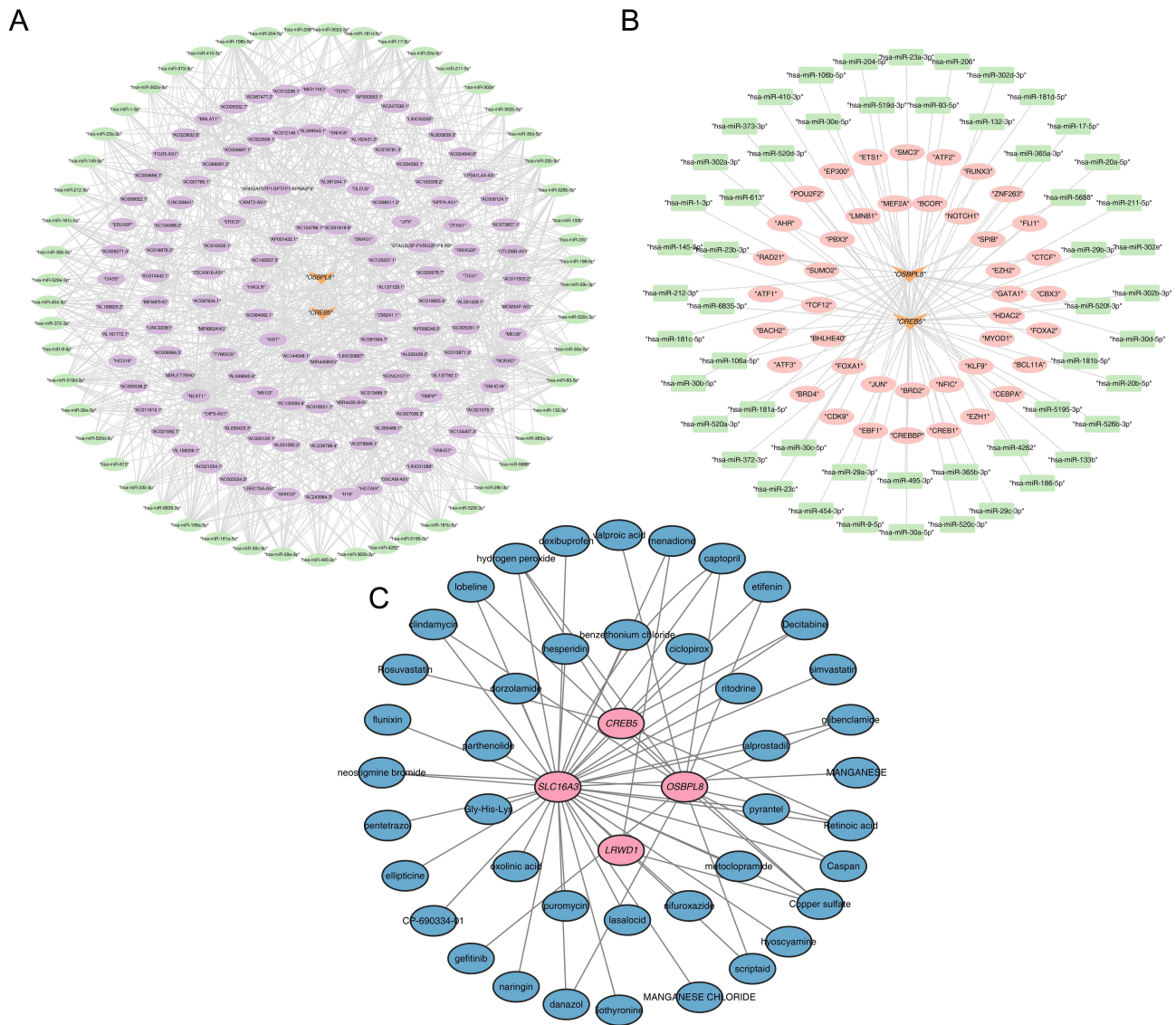


Figure 6 The ceRNA regulatory network analysis, TF-mRNA-miRNA network construction and drug prediction results. **(A)** A Map of a ceRNA network constructed by *OSBP18* and *CREB5*; **(B)** TF-mRNA-miRNA regulatory network; **(C)** A targeted drug prediction map for DPN treatment based on *OSBP18* and *CREB5*.

diabetes mellitus.⁴⁶ Specifically, this study demonstrates a causal relationship between *OSBP18* and DPN. We speculate that *OSBP18* may affect DPN through the miR-143-ORP8 pathway.

SLC16A3 (MCT4) belongs to the monocarboxylate transporter (MCT) family, facilitating the transport of pH-dependent monocarboxylates such as lactic acid and pyruvic acid.⁴⁷ Recent investigations indicate that lactic acid enhances neuronal mitochondrial metabolism and energy generation in peripheral nerves.⁴⁸ DPN apparently involves metabolic dysfunction and energy depletion of multiple cells within the peripheral nervous system, implying a robust association between *SLC16A3* and DPN. Moreover, the spatial distribution of MCT within the peripheral nervous system (PNS) hints at its potential involvement in lactic acid transport and myelination.⁴⁹ Notably, a study revealed that the experimental exacerbation of DPN was associated with a reduction in monocarboxylate transporter-1 (MCT1).⁵⁰

CREB5 is a member of the cAMP-response element binding (CREB) protein gene family and is classified under the ATF2 subfamily. This subgroup demonstrates a heightened affinity for cAMP-response elements (CREs) and participates in diverse cellular functions such as survival, proliferation, and glucose metabolism.⁵¹ Recent studies have suggested a potential protective role for activated *CREB5* in shielding diabetic proximal renal tubule cells from apoptosis.⁵² Additionally, *CREB5* has been associated with the AMPK signaling pathway,⁵³ which is speculated to be pivotal in the

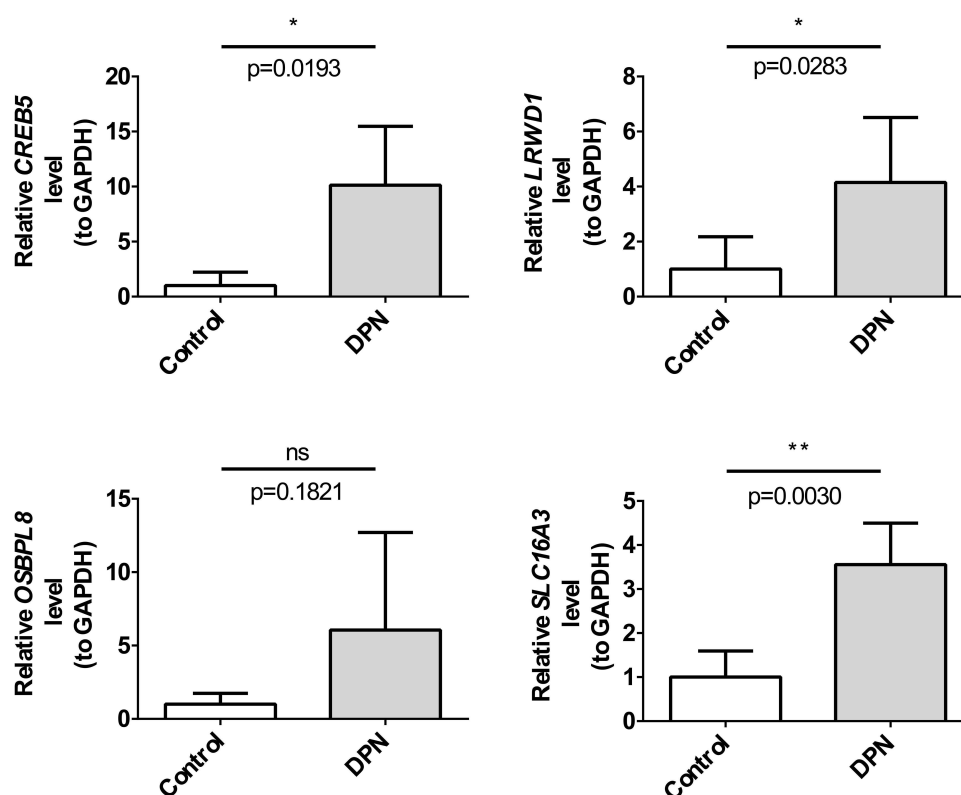


Figure 7 The expression results verified by RT-qPCR. *: $P < 0.05$, **: $P < 0.01$, ns, no significance.

pathogenesis of DPN. AMPK-mediated mitochondrial impairment in Schwann cells may instigate demyelination and axonal atrophy, both implicated in the development of the disease.⁵⁴

LRWD1 is an origin recognition complex (ORC)-associated protein that plays a key role in heterochromatin replication in mammalian cells by recruiting promoter ORCs.⁵⁵ Few previous studies have associated it with diabetes-related diseases, and this study is the first to find an association between *LRWD1* and DPN.

Based on our differential analysis, four candidate biomarkers, *CREB5*, *LRWD1*, *OSBPL8*, and *SLC16A3*, exhibited significant differential upregulation. Moreover, beyond the causal relationships found by MR, the consistency of their expression trends was verified in both the training and validation sets. Given these insights, these genes emerge as promising targets for therapeutic intervention in DPN. Further investigation into their molecular mechanisms is imperative to enhance our understanding and unlock their therapeutic potential.

Of particular interest in our GO analysis was toll-like receptor binding. Toll-like receptors (TLRs) are pivotal proteins in the innate immune response, initiating a signaling cascade upon interaction with microbial pathogen-expressed TLR ligands. This cascade leads to the production of cytokine and the initiation of adaptive immune responses. Dysregulated immune mechanisms play a crucial role in the pathogenesis of DPN.⁵⁶ Among the TLR, *TLR4* plays a crucial role in inflammatory diseases.⁵⁷ DPN is increasingly recognized as a chronic inflammatory condition wherein *TLR4* expression in dorsal root ganglia can be induced by high glucose, free fatty acids, and angiotensin II. This induction activates downstream signaling pathways of inflammation, leading to the activation of NF- κ B and the subsequent production of inflammatory factors such as TNF- α , prostaglandins, and activated cyclooxygenase (COX), thereby instigating neuroinflammation in DPN.⁵⁸ Notably, the Toll-like receptor signaling pathway was similarly enriched in our KEGG results. Moreover, *TLR4* has been identified as a potentially sensitive diagnostic biomarker for DPN in patients with type 2 diabetes.⁵⁷ This evidence underscores the significant role of Toll-like receptors in the progression of DPN and suggests that DEGs may influence DPN through the Toll-like receptor signaling pathway.

Our biomarkers underwent further analysis using GSEA to elucidate their molecular mechanisms. They were notably enriched in pathways related to metabolic reactions of amino acids and derivatives, rRNA processing, and translation. While the metabolism of amino acids and their derivatives in DPN has been scarcely described, studies have highlighted their significance in relevant pathways in diabetic foot ulcers (DFU). Furthermore, literature has underscored a significant association between DPN and DFU,⁵⁹ with DPN serving as a significant initiating risk factor for DFU development.⁶⁰ Although a causal relationship between the two variables was not established in our study, it's worth noting their interconnectedness. Moreover, GSVA analyses revealed enrichment of the NF- κ B pathway, consistent with the potential for neuroinflammation in DPN via the production of inflammatory factors. This further underscores the importance of the signaling pathways involving key genes in DPN progression. Additionally, *CREB5* is markedly activated in proximal renal tubular epithelial cells of diabetic patients⁵² and has been found to regulate the MET signaling pathway crucial for colorectal cancer metastasis.⁶¹ *OSBPL8* overexpression has been observed in cholangiocarcinomas.⁶² *SLC16A3* is abnormally upregulated at the plasma membrane of cardiomyocytes from patients with type 2 diabetes⁶³ and its role in intracellular pH regulation and lactate-based metabolism has been explored in various cancers, including colorectal, breast, and lung cancers.⁶⁴ In summary, these biomarkers are not only implicated in the pathogenesis of DPN and diabetes-related diseases but also play roles in cancer, providing potential avenues for the treatment of related cancers.

In order to delve into the genes linked with biomarkers functions and elucidate the functional correlations among different genes, we conducted GeneMANIA analysis alongside functional correlation analysis. GeneMANIA analysis revealed that *LRWD1* interacts most closely with *ORC5* and *ORC2*. *LRWD1* interacts directly with the N-terminus of *ORC2*, and the stability of *LRWD1* depends on its binding to *ORC2*.⁶⁵ The interaction of *LRWD1* with *ORC5* has been rarely mentioned in previous studies. Notably, the functional similarity among these four biomarkers was observed to be modest. Furthermore, we undertook subcellular localization analysis and predicted m6A binding sites for the biomarkers to gain deeper insights into their roles. The subcellular localization provides important information about the function and activity of biomarkers in the cell. DNA methylation of the *SLC16A3* promoter regulates MCT4 expression and affects clinical outcomes in renal cancer.⁶⁶ Hypomethylation of *CREB5* upregulates *CREB5*, thereby altering trophoblast cell function.⁶⁷ Thus, m6A binding site prediction results indicate that m6A methylation of these genes at different base positions may have an impact on their function and regulation. It provides important guidance and insights for further studies in the future.

To delve deeper into the functions and regulatory mechanisms of the biomarkers, we analyzed competing endogenous RNA (ceRNA) regulatory networks. In this regard, we identified 54 miRNA target genes and predicted 759 lncRNA target genes based on these miRNAs to construct a lncRNA-miRNA-key gene regulatory network. Notably, HSA-miR-23a-3p, a member of a major miRNA family involved in regulating T-cell immune responses, exhibited significant reduction in diabetic patients. Inhibition of the NF- κ B pathway by HSA-miR-23a-3p has been shown to suppress the expression of pro-inflammatory molecules and angiogenic potential, potentially ameliorating neuroinflammation in DPN.⁶⁸ Additionally, miR-23a has been implicated in inhibiting high glucose-induced inflammation in microglia by down-regulating *PDE4B*, attenuating DPN.⁶⁹ Moreover, in individuals with type 1 diabetes and long-term metabolic syndrome, HSA-miR-495-3p is downregulated, and previous studies have linked this miRNA to immune and inflammatory responses.⁷⁰ Notably, in patients with DFU, tissue-specific expression of miR-23a and miR-23b was low, while miR-23c was elevated.⁷¹ Considering the association of DPN with DFU, we posit that HSA-miR-23a-3p, HSA-miR-495-3p, HSA-miR-23b-3p and HSA-miR-23c could potentially be ceRNA pathways implicated in DPN regulation. However, further experiments are warranted to confirm this hypothesis.

Additionally, we constructed a transcription factor (TF) regulatory network of key genes to explore the relationships between transcription factors, miRNAs, and key genes. Predicted TFs by *OSBPL8* and *CREB5* included *PBX3*, *ETS1*, *EP300*, *CREBBP*, and *BRD4*. Among them, *CREBBP* and *EP300* have been found to be significant for DPN diagnosis, potentially affecting DPN by influencing lipid metabolism toxicity or inflammatory processes triggered by inflammatory stimuli.⁷² Furthermore, *BRD4* plays a pivotal role in the pathogenesis of high glucose-induced cardiomyocyte hypertrophy through the AKT pathway.⁷³ Based on existing studies, it's evident that some predicted transcription factors are indeed involved in DPN regulation, shedding light on the pathogenesis of DPN. This offers new perspectives and clues for a comprehensive understanding of DPN pathogenesis.

In addition, we conducted drug predictions for the four biomarkers, yielding a total of 43 potential drugs. Among these, examples include Rosuvastatin and Neostigmine Bromide. Studies have recognized that Rosuvastatin may alleviate DPN through its anti-fibrotic synergy.⁷⁴ Neostigmine bromide functions by inhibiting the enzymatic cleavage of acetylcholine, thereby reversibly inhibiting acetylcholinesterase. Consequently, it can persist in cholinergic nerve endings for an extended period, eliciting an excitatory effect on smooth and skeletal muscles. Furthermore, we substantiated biomarker expression through RT-qPCR, with outcomes aligning consistently with the observed trends across the two datasets employed in our study. Four biomarkers were highly expressed in the DPN group, with only *OSBPL8* showing a non-significant difference between groups. This observation may be attributed to the constrained sample size utilized for RT-qPCR validation.

It is noteworthy that the present study has certain limitations that warrant attention in subsequent research. Our analysis was conducted using retrospective data derived from public datasets, which may introduce case selection bias and limit the generalizability of our findings. Consequently, the diagnostic and predictive utility of biomarkers in DPN requires further validation through large-scale clinical trials. Additionally, the regulatory mechanisms of these biomarkers in DPN need to be further elucidated through functional and mechanistic studies.

Conclusion

In conclusion, our study leveraged transcriptomic analysis to pinpoint genes exhibiting significant differential expression between disease and control groups. Subsequently, we employed both univariate and multivariate MR studies. This allowed us to elucidate the causal relationships between DE-DPN-RGs and DPN, yielding more reliable findings and the identification of four potential biomarkers related to DPN: *SLC16A3*, *CREB5*, *OSBPL8* and *LRWD1*. Moving forward, we intend to closely monitor the progress of these biomarkers and targeted drugs. Our study possesses several noteworthy limitations that warrant consideration. First, the clinical utility of biomarkers necessitates validation across diverse patient populations. Moreover, the targeted drugs identified in our study require thorough validation through extensive clinical trials before obtaining approval for clinical application. Ultimately, our findings offer new insights into the prevention and treatment of DPN, paving the way for novel strategies and directions in early diagnosis.

Abbreviations

DPN, diabetic peripheral neuropathy; MR, mendelian randomization; DEGs, differentially expressed genes; DE-DPN-RGs, DPN-related differentially expressed genes; RT-qPCR, reverse transcription quantitative polymerase chain reaction; LS, least squares; NE, not estimable; IVs, instrumental variables; NCS, nerve conduction studies; GEO, gene expression omnibus; eQTL, expression quantitative trait locus; SNPs, single nucleotide polymorphisms; FC, fold-change; GO, gene ontology; KEGG, kyoto encyclopedia of genes and genomes; PPI, protein-protein interaction; LD, linkage disequilibrium; MVMR, multivariable mendelian randomization; WM, weighted median; MR Egger, mendelian randomization egger regression; OR, odds ratio; GSEA, gene set enrichment analysis; SRAMP, sequence-based RNA adenosine methylation site predictor database; miRDB, a database for microRNA target prediction; TargetScan, a computational tool for predicting microRNA targets; Starbase, a database for analyzing noncoding RNA interactions; ceRNA, competing endogenous RNA; TF, transcription factor; DsigDB, drug signatures database; FADD, fas-associated protein with death domain; RIP1, receptor-interacting protein kinase 1; CLEC7A, c-type lectin domain family 7 member A; NFAT, nuclear factor of activated T-cells; FGFR4, fibroblast growth factor receptor 4; PI3K, phosphatidylinositol 3-kinase; ORC5 and ORC2, origin recognition complex subunits 5 and 2; CREB5, cAMP response element binding protein 5; LRWD1, leucine rich WD repeat containing 1; OSBPL8, oxysterol binding protein like 8.

Data Sharing Statement

The datasets [GSE95849 and GSE185011] for this study can be found in [the Gene Expression Omnibus (GEO)] [<https://www.ncbi.nlm.nih.gov/geo>]. The datasets [finn-b-DM_NEUROPATHY] for this study can be found in [IEU OpenGWAS] [<https://gwas.mrcieu.ac.uk/>].

Ethics Approval and Informed Consent

The study was conducted in accordance with the Declaration of Helsinki, and approved by the Medical Ethics Committee of Zunyi Medical University (protocol code [2022] 1-063 and date of approval: March 7, 2022).

Consent to Participate

Participants in this study were given a detailed and clear explanation of the research aims, methods, potential risks, and benefits. They were informed that their participation was entirely voluntary and that they could withdraw from the study at any time. They were also offered the opportunity to ask questions and provided written informed consent before joining the study.

Acknowledgments

We would like to express our sincere gratitude to all individuals and organizations who supported and assisted us throughout this research.

Funding

This research was funded by the National Natural Science Foundation of China, grant number 82260167 and 82460167; Guizhou Science and Technology Association Youth Science and Technology Talent Promotion Project (No. GASTYESS202434); Science and Technology Planning Project of Guizhou Province, grant number Guizhou department combine basics-ZK[2022] General 639; Kweichow Moutai Hospital science and technology innovation project by MTyk2022-42.

Disclosure

The authors declare that they have no competing interests in this work.

References

- Zimmet P, Alberti KG, Magliano DJ, Bennett PH. Diabetes mellitus statistics on prevalence and mortality: facts and fallacies. *Nat Rev Endocrinol.* 2016;12(10):616–622. doi:10.1038/nrendo.2016.105
- Magliano DJ, Boyko EJ. IDF Diabetes Atlas. 2021.
- Hicks CW, Selvin E. Epidemiology of Peripheral Neuropathy and Lower Extremity Disease in Diabetes. *Curr Diab Rep.* 2019;19(10):86. doi:10.1007/s11892-019-1212-8
- Singh R, Kishore L, Kaur N. Diabetic peripheral neuropathy: current perspective and future directions. *Pharmacol Res.* 2014;80:21–35. doi:10.1016/j.phrs.2013.12.005
- Edwards JL, Vincent AM, Cheng HT, Feldman EL. Diabetic neuropathy: mechanisms to management. *Pharmacol Ther.* 2008;120(1):1–34. doi:10.1016/j.pharmthera.2008.05.005
- Elafros MA, Andersen H, Bennett DL, et al. Towards prevention of diabetic peripheral neuropathy: clinical presentation, pathogenesis, and new treatments. *Lancet Neurol.* 2022;21(10):922–936. doi:10.1016/S1474-4422(22)00188-0
- Yu Y. Gold Standard for Diagnosis of DPN. *Front Endocrinol.* 2021;12:719356. doi:10.3389/fendo.2021.719356
- Selvarajah D, Kar D, Khunti K, et al. Diabetic peripheral neuropathy: advances in diagnosis and strategies for screening and early intervention. *Lancet Diabetes Endocrinol.* 2019;7(12):938–948. doi:10.1016/S2213-8587(19)30081-6
- Li W, Wang R, Wang W. Exploring the causality and pathogenesis of systemic lupus erythematosus in breast cancer based on Mendelian randomization and transcriptome data analyses. *Front Immunol.* 2022;13:1029884. doi:10.3389/fimmu.2022.1029884
- Smith GD, Lawlor DA, Harbord R, Timpson N, Day I, Ebrahim S. Clustered environments and randomized genes: a fundamental distinction between conventional and genetic epidemiology. *PLoS Med.* 2007;4(12):e352. doi:10.1371/journal.pmed.0040352
- Zhang Y, Tang Z, Tong L, Wang Y, Li L. Serum uric acid and risk of diabetic neuropathy: a genetic correlation and mendelian randomization study. *Front Endocrinol.* 2023;14:1277984. doi:10.3389/fendo.2023.1277984
- Zou L, Zhu D, Gong M, Yu J. The influence of genetic predisposition to oxidative stress on painful diabetic peripheral neuropathy: a mendelian randomization study. *Cell Mol Bio.* 2024;70(3):168–173.
- Soares L, Villalba Silva GC, Kubaski F, Giugliani R, Matte U. MPSBase: comprehensive repository of differentially expressed genes for mucopolysaccharidoses. *Mol Genet Metab.* 2021;133(4):372–377. doi:10.1016/j.ymgme.2021.06.004
- Luo L, Zhou WH, Cai JJ, et al. Gene Expression Profiling Identifies Downregulation of the Neurotrophin-MAPK Signaling Pathway in Female Diabetic Peripheral Neuropathy Patients. *J Diabetes Res.* 2017;2017:8103904. doi:10.1155/2017/8103904
- Hui Z, Chen YM, Gong WK, et al. Shared and specific biological signalling pathways for diabetic retinopathy, peripheral neuropathy and nephropathy by high-throughput sequencing analysis. *Diab Vasc Dis Res.* 2022;19(4):14791641221122918. doi:10.1177/14791641221122918
- Yuan JX, Jiang Q, Yu SJ. Diabetes mellitus and prostate cancer risk: a mendelian randomization analysis. *World J Diabetes.* 2023;14(12):1839–1848. doi:10.4239/wjd.v14.i12.1839

17. Ritchie ME, Phipson B, Wu D, et al. limma powers differential expression analyses for RNA-sequencing and microarray studies. *Nucleic Acids Res.* 2015;43(7):e47. doi:10.1093/nar/gkv007
18. He Z, Jiang Q, Li F, Chen M. Crosstalk between Venous Thromboembolism and Periodontal Diseases: a Bioinformatics Analysis. *Dis Markers.* 2021;2021:1776567. doi:10.1155/2021/1776567
19. Karobari MI, Batul R, Khan M, et al. Micro computed tomography (Micro-CT) characterization of root and root canal morphology of mandibular first premolars: a systematic review and meta-analysis. *BMC Oral Health.* 2024;24(1):1. doi:10.1186/s12903-023-03624-5
20. Wang M, Fu L, Tian J, Zhang Y, Rossi L, Wang K. Function and prognosis analysis of nucleolus protein DCAF13 in breast cancer. *Transl Cancer Res.* 2023;12(12):3744–3751. doi:10.21037/tcr-23-1923
21. Yu G, Wang LG, Han Y, He QY. clusterProfiler: an R package for comparing biological themes among gene clusters. *OMICS.* 2012;16(5):284–287. doi:10.1089/omi.2011.0118
22. Beckman MF, Brennan EJ, Igba CK, Brennan MT, Mougeot FB, Mougeot JC. A Computational Text Mining-Guided Meta-Analysis Approach to Identify Potential Xerostomia Drug Targets. *J Clin Med.* 2022;11(5):1442. doi:10.3390/jcm11051442
23. Shannon P, Markiel A, Ozier O, et al. Cytoscape: a software environment for integrated models of biomolecular interaction networks. *Genome Res.* 2003;13(11):2498–2504. doi:10.1101/gr.1239303
24. Burgess S, Thompson SG. Interpreting findings from Mendelian randomization using the MR-Egger method. *Eur J Epidemiol.* 2017;32(5):377–389. doi:10.1007/s10654-017-0255-x
25. Hemani G, Tilling K, Davey Smith G. Orienting the causal relationship between imprecisely measured traits using GWAS summary data. *PLoS Genet.* 2017;13(11):e1007081. doi:10.1371/journal.pgen.1007081
26. Burgess S, Scott RA, Timpson NJ, Davey Smith G, Thompson SG. Using published data in Mendelian randomization: a blueprint for efficient identification of causal risk factors. *Eur J Epidemiol.* 2015;30(7):543–552. doi:10.1007/s10654-015-0011-z
27. Bowden J, Davey Smith G, Haycock PC, Burgess S. Consistent Estimation in Mendelian Randomization with Some Invalid Instruments Using a Weighted Median Estimator. *Genet Epidemiol.* 2016;40(4):304–314. doi:10.1002/gepi.21965
28. Bowden J, Davey Smith G, Burgess S. Mendelian randomization with invalid instruments: effect estimation and bias detection through Egger regression. *Int J Epidemiol.* 2015;44(2):512–525. doi:10.1093/ije/dyv080
29. Hemani G, Zheng J, Elsworth B, et al. The MR-Base platform supports systematic causal inference across the human phenome. *Elife.* 2018;7:e34408. doi:10.7554/eLife.34408
30. Hartwig FP, Davey Smith G, Bowden J. Robust inference in summary data Mendelian randomization via the zero modal pleiotropy assumption. *Int J Epidemiol.* 2017;46(6):1985–1998. doi:10.1093/ije/dyx102
31. Duan X, Xing F, Zhang J, et al. Bioinformatic analysis of related immune cell infiltration and key genes in the progression of osteonecrosis of the femoral head. *Front Immunol.* 2023;14:1340446. doi:10.3389/fimmu.2023.1340446
32. Wu T, Hu E, Xu S, et al. clusterProfiler 4.0: a universal enrichment tool for interpreting omics data. *Innovation.* 2021;2(3):100141. doi:10.1016/j.xinn.2021.100141
33. Guo L, Yuan M, Jiang S, Jin G, Li P. Expression of pyroptosis-associated genes and construction of prognostic model for thyroid cancer. *Transl Cancer Res.* 2023;12(12):3360–3383. doi:10.21037/tcr-23-810
34. Hu Y, Wu Y, Gan F, et al. Identification of Potential Therapeutic Target Genes in Osteoarthritis. *Evid Based Complement Alternat Med.* 2022;2022:8027987. doi:10.1155/2022/8027987
35. Tang Q, Nie F, Kang J, Chen W. mRNALocator: enhance the prediction accuracy of eukaryotic mRNA subcellular localization by using model fusion strategy. *Mol Ther.* 2021;29(8):2617–2623. doi:10.1016/j.ymthe.2021.04.004
36. Hu A, Nussbaum YI, Mitchem J, Yoo J. Colorectal Cancer-Associated Myofibroblasts Exhibit Enhanced Angiogenesis and Signaling via the PLXNB2 Receptor. *J Surg Res.* 2024;296:273–280. doi:10.1016/j.jss.2023.12.036
37. Yan BR, Wang P, Li YS, et al. Roles and mechanisms of m(6)A modification regulating RP11-426A6.5 in laryngeal squamous cell carcinoma. *Zhonghua Er Bi Yan Hou Tou Jing Wai Ke Za Zhi.* 2022;57(12):1470–1478. doi:10.3760/cma.j.cn115330-20220313-00111
38. Wong N, Wang X. miRDB: an online resource for microRNA target prediction and functional annotations. *Nucleic Acids Res.* 2015;43(Database issue):D146–52. doi:10.1093/nar/gku1104
39. Li H, Liang J, Wang J, et al. Mex3a promotes oncogenesis through the RAS1/MAPK signaling pathway in colorectal cancer and is inhibited by hsa-miR-6887-3p. *Cancer Commun.* 2021;41(6):472–491. doi:10.1002/cac2.12149
40. Liu J, Fan Y, Song R, et al. Prostatitis No.1 traditional Chinese medicine significantly exhibited anti-inflammation role on prostatitis through miR-205-5p/YES1. *Cell Mol Bio.* 2023;69(15):270–276. doi:10.14715/cmb/2023.69.15.45
41. Tram V, Khoa Ta HD, Anuraga G, et al. Dysbindin Domain-Containing 1 in Prostate Cancer: new Insights into Bioinformatic Validation of Molecular and Immunological Features. *Int J Mol Sci.* 2023;24(15):11930. doi:10.3390/ijms241511930
42. Zhang GZ, Li L, Luo ZB, Zhang CY, Wang YG, Kang XW. Identification and experimental validation of key extracellular proteins as potential targets in intervertebral disc degeneration. *Bone Joint Res.* 2023;12(9):522–535. doi:10.1302/2046-3758.129.BJR-2022-0369.R2
43. Yang K, Wang Y, Li YW, et al. Progress in the treatment of diabetic peripheral neuropathy. *Biomed Pharmacother.* 2022;148:112717. doi:10.1016/j.biopha.2022.112717
44. Olkkonen VM. OSBP-Related Protein Family in Lipid Transport Over Membrane Contact Sites. *Lipid Insights.* 2015;8(Suppl 1):1–9. doi:10.4137/LPLI.S31726
45. Santos NC, Girik V, Nunes-Hasler P. ORP5 and ORP8: sterol Sensors and Phospholipid Transfer Proteins at Membrane Contact Sites. *Biomolecules.* 2020;10(6):928. doi:10.3390/biom10060928
46. Jordan SD, Krüger M, Willmes DM, et al. Obesity-induced overexpression of miRNA-143 inhibits insulin-stimulated AKT activation and impairs glucose metabolism. *Nat Cell Biol.* 2011;13(4):434–446. doi:10.1038/ncb2211
47. Pinheiro C, Longatto-Filho A, Azevedo-Silva J, Casal M, Schmitt FC, Baltazar F. Role of monocarboxylate transporters in human cancers: state of the art. *J Bioenerg Biomembr.* 2012;44(1):127–139. doi:10.1007/s10863-012-9428-1
48. Jia L, Liao M, Mou A, et al. Rheb-regulated mitochondrial pyruvate metabolism of Schwann cells linked to axon stability. *Dev Cell.* 2021;56(21):2980–2994.e6. doi:10.1016/j.devcel.2021.09.013
49. Domènech-Estévez E, Baloui H, Repond C, et al. Distribution of monocarboxylate transporters in the peripheral nervous system suggests putative roles in lactate shuttling and myelination. *J Neurosci.* 2015;35(10):4151–4156. doi:10.1523/JNEUROSCI.3534-14.2015

50. Jha MK, Ament XH, Yang F, et al. Reducing monocarboxylate transporter MCT1 worsens experimental diabetic peripheral neuropathy. *Exp Neurol.* 2020;333:113415. doi:10.1016/j.expneurol.2020.113415
51. Konkright MD, Montminy M. CREB: the unindicted cancer co-conspirator. *Trends Cell Biol.* 2005;15(9):457–459. doi:10.1016/j.tcb.2005.07.007
52. Shi W, Le W, Tang Q, Shi S, Shi J. Regulon analysis identifies protective FXR and CREB5 in proximal tubules in early diabetic kidney disease. *BMC Nephrol.* 2023;24(1):180. doi:10.1186/s12882-023-03239-6
53. Hong EH, Yeom H, Yu HS, et al. Genome-wide association study of the response of patients with diabetic macular edema to intravitreal Anti-VEGF injection. *Sci Rep.* 2022;12(1):22527. doi:10.1038/s41598-022-26048-7
54. Zhang Q, Song W, Zhao B, et al. Quercetin Attenuates Diabetic Peripheral Neuropathy by Correcting Mitochondrial Abnormality via Activation of AMPK/PGC-1 α Pathway in vivo and in vitro. *Front Neurosci.* 2021;15:636172. doi:10.3389/fnins.2021.636172
55. Bartke T, Vermeulen M, Xhemalce B, Robson SC, Mann M, Kouzarides T. Nucleosome-interacting proteins regulated by DNA and histone methylation. *Cell.* 2010;143(3):470–484. doi:10.1016/j.cell.2010.10.012
56. Mu ZP, Wang YG, Li CQ, et al. Association Between Tumor Necrosis Factor- α and Diabetic Peripheral Neuropathy in Patients with Type 2 Diabetes: a Meta-Analysis. *Mol Neurobiol.* 2017;54(2):983–996. doi:10.1007/s12035-016-9702-z
57. Zhu T, Meng Q, Ji J, Lou X, Zhang L. Toll-like receptor 4 and tumor necrosis factor- α as diagnostic biomarkers for diabetic peripheral neuropathy. *Neurosci Lett.* 2015;585:28–32. doi:10.1016/j.neulet.2014.11.020
58. Aghamiri SH, Komlakh K, Ghaffari M. The crosstalk among TLR2, TLR4 and pathogenic pathways; a treasure trove for treatment of diabetic neuropathy. *Inflammopharmacology.* 2022;30(1):51–60. doi:10.1007/s10787-021-00919-3
59. Nowak NC, Menichella DM, Miller R, Paller AS. Cutaneous innervation in impaired diabetic wound healing. *Transl Res.* 2021;236:87–108. doi:10.1016/j.trsl.2021.05.003
60. Boulton AJ, Vileikyte L, Ragnarson-Tennvall G, Apelqvist J. The global burden of diabetic foot disease. *Lancet.* 2005;366(9498):1719–1724. doi:10.1016/S0140-6736(05)67698-2
61. Wang S, Qiu J, Liu L, et al. CREB5 promotes invasiveness and metastasis in colorectal cancer by directly activating MET. *J Exp Clin Cancer Res.* 2020;39(1):168. doi:10.1186/s13046-020-01673-0
62. Loilome W, Wechagama P, Namwat N, et al. Expression of oxysterol binding protein isoforms in opisthorchiasis-associated cholangiocarcinoma: a potential molecular marker for tumor metastasis. *Parasitol Int.* 2012;61(1):136–139. doi:10.1016/j.parint.2011.07.003
63. Ma XM, Geng K, Wang P, Jiang Z, Law BY, Xu Y. MCT4-dependent lactate transport: a novel mechanism for cardiac energy metabolism injury and inflammation in type 2 diabetes mellitus. *Cardiovasc Diabetol.* 2024;23(1):96. doi:10.1186/s12933-024-02178-2
64. Baek G, Tse YF, Hu Z, et al. MCT4 defines a glycolytic subtype of pancreatic cancer with poor prognosis and unique metabolic dependencies. *Cell Rep.* 2014;9(6):2233–2249. doi:10.1016/j.celrep.2014.11.025
65. Shen Z, Chakraborty A, Jain A, et al. Dynamic association of ORCA with prereplicative complex components regulates DNA replication initiation. *Mol Cell Biol.* 2012;32(15):3107–3120. doi:10.1128/MCB.00362-12
66. Fisel P, Kruck S, Winter S, et al. DNA methylation of the SLC16A3 promoter regulates expression of the human lactate transporter MCT4 in renal cancer with consequences for clinical outcome. *Clin Cancer Res.* 2013;19(18):5170–5181. doi:10.1158/1078-0432.CCR-13-1180
67. Yu M, Du G, Xu Q, et al. Integrated analysis of DNA methylome and transcriptome identified CREB5 as a novel risk gene contributing to recurrent pregnancy loss. *EBioMedicine.* 2018;35:334–344. doi:10.1016/j.ebiom.2018.07.042
68. Markopoulos GS, Roupakia E, Tokamani M, et al. Roles of NF- κ B Signaling in the Regulation of miRNAs Impacting on Inflammation in Cancer. *Biomedicines.* 2018;6(2):40. doi:10.3390/biomedicines6020040
69. Zhang X, Xia L, Xie A, Liao O, Ju F, Zhou Y. Low concentration of Bupivacaine ameliorates painful diabetic neuropathy by mediating miR-23a/PDE4B axis in microglia. *Eur J Pharmacol.* 2021;891:173719. doi:10.1016/j.ejphar.2020.173719
70. Swolin-Eide D, Forsander G, Pundziute Lyckå A, et al. Circulating microRNAs in young individuals with long-duration type 1 diabetes in comparison with healthy controls. *Sci Rep.* 2023;13(1):11634. doi:10.1038/s41598-023-38615-7
71. Amin KN, Umapathy D, Anandharaj A, et al. miR-23c regulates wound healing by targeting stromal cell-derived factor-1 α (SDF-1 α /CXCL12) among patients with diabetic foot ulcer. *Microvasc Res.* 2020;127:103924. doi:10.1016/j.mvr.2019.103924
72. Yang Y, Wang Q. Three genes expressed in relation to lipid metabolism considered as potential biomarkers for the diagnosis and treatment of diabetic peripheral neuropathy. *Sci Rep.* 2023;13(1):8679. doi:10.1038/s41598-023-35908-9
73. Wang Q, Sun Y, Li T, et al. Function of BRD4 in the pathogenesis of high glucose-induced cardiac hypertrophy. *Mol Med Rep.* 2019;19(1):499–507. doi:10.3892/mmr.2018.9681
74. El-Sawaf ES, Saleh S, Abdallah DM, Ahmed KA, El-Abhar HS. Vitamin D and rosuvastatin obliterate peripheral neuropathy in a type-2 diabetes model through modulating Notch1, Wnt-10 α , TGF- β and NRF-1 crosstalk. *Life Sci.* 2021;279:119697. doi:10.1016/j.lfs.2021.119697

International Journal of General Medicine

Publish your work in this journal

The International Journal of General Medicine is an international, peer-reviewed open-access journal that focuses on general and internal medicine, pathogenesis, epidemiology, diagnosis, monitoring and treatment protocols. The journal is characterized by the rapid reporting of reviews, original research and clinical studies across all disease areas. The manuscript management system is completely online and includes a very quick and fair peer-review system, which is all easy to use. Visit <http://www.dovepress.com/testimonials.php> to read real quotes from published authors.

Submit your manuscript here: <https://www.dovepress.com/international-journal-of-general-medicine-journal>

Dovepress
Taylor & Francis Group